

# A New Method for Rotor Time Constant Tuning in Indirect Field Oriented Control

Julio C. Moreira, *Member, IEEE*, and Thomas A. Lipo

**Abstract**—The purpose of this paper is to investigate and implement a new adaptive controller for correction of the rotor time constant used in the calculation of the slip frequency in Indirect Field Oriented Control (IFOC) of induction machines. The implementation of the controller is based on the machine air gap flux which is measured by detecting the third harmonic component of the stator phase voltages. The proposed adaptive controller depends only on a single, easily measurable machine parameter estimate, namely the magnetizing inductance. Moreover, a correction strategy to compensate for changes of the magnetizing inductance when changes in the air gap flux level occur is also proposed in this paper. Such strategy is based on a function that relates the value of this inductance to the amplitude of the third harmonic stator voltage component. This new controller does not require any sensors in the air gap of the machine nor does it require complex computations. Only access to the stator neutral connection is necessary to measure the air gap flux. Verification of the validity and feasibility of the technique is obtained from simulation and experimental results.

## I. INTRODUCTION

MANY methods presented in recent literature have been proposed to circumvent the problem of detuning of the slip calculator gain of indirect field oriented controlled induction machines [1]–[7]. Identification, estimation, and adaptation schemes have been employed in these works with the sole intent to correct the rotor time constant used as a reference value in the calculation of the slip frequency. In the majority of these studies, the rotor time constant is corrected by means of schemes that depend upon a multitude of other machine parameters such as the magnetizing inductance, stator and/or rotor leakage inductances and even on the stator winding resistance.

A Model Reference Adaptive Controller (MRAC) is proposed and implemented in this work. The dependance of the MRAC on machine parameters can be minimized when a convenient machine variable is chosen to be the reference model. In this sense, the rotor flux would be the ideal variable to measure and utilize in the correction for variations of the rotor time constant without the need of any machine parameter. Such a procedure, however, requires the installation of Hall-Effect sensors to measure the rotor flux which would preclude the utilization of the indirect type of field orientation here proposed since it would then be more desirable to simply

implement a Direct Field Orientation controller. The next variable closest to the ideal case represented by the choice of the rotor flux, is the air gap flux. With the air gap flux one needs only the knowledge of the magnetizing inductance of the machine to establish an adaptive controller for the rotor time constant.

It is shown in this paper that a third harmonic air gap flux component exists due to the saturation of the stator magnetic material. This harmonic flux component induces a third harmonic zero sequence voltage component in the stator phases that is a function of the amplitude of the air gap flux and the winding configuration of the stator phases. When the three phase voltages are summed, the fundamental and characteristic harmonics are cancelled and the resultant waveform contains mainly a third harmonic and higher frequency components due to the rotor slots [8], [9].

The method described in this paper proposes an original approach to measure the air gap flux from the third harmonic contents of the stator voltages. An adaptive scheme is implemented which will at the same time adapt for rotor time constant, as well as magnetizing inductance estimates. The air gap flux measured from the third harmonic contents of the stator phase voltages is resolved into its  $d$  and  $q$  components, with the  $d$  component being utilized in the adaption scheme for the rotor time constant while the magnitude of the flux adapts the magnetizing inductance estimate.

## II. MEASUREMENT OF AIR GAP FLUX FROM THE THIRD HARMONIC CONTENTS OF MACHINE PHASE VOLTAGE

The MRAC developed is based on the estimation of the  $d$ -axis air gap flux component that is obtained, in turn, from the third harmonic content of the stator phase voltages. A brief discussion of the machine operating principles introducing the method of measuring the air gap flux devised in this research is presented in [8] and [9]. Therein, the authors demonstrate that a dominant third harmonic air gap flux component is produced in the air gap as a consequence that the stator teeth of the machine are normally (as a machine design option) operating in a saturated condition. As the stator teeth begin to saturate, the teeth with the highest flux density will saturate first so that the flux distribution around the air gap will assume a flattened sinusoidal form with peak value  $B_{sat}$  as shown in Fig. 1.

The flattening of the air gap flux is produced primarily by a third harmonic component that is originated by the non-linear characteristic of the magnetic material utilized in the machine. The air gap flux will have, at any instant, the same spatial distribution around the air gap provided that the machine

Manuscript received November 23, 1991; revised April 17, 1993.

J. C. Moreira is with the Elisha Gray II Research and Engineering Center, Whirlpool Corporation, Benton Harbor, MI 49022.

T. A. Lipo is with the Electrical and Computer Engineering Department, University of Wisconsin, Madison, WI 53705.

IEEE Log Number 9211688.

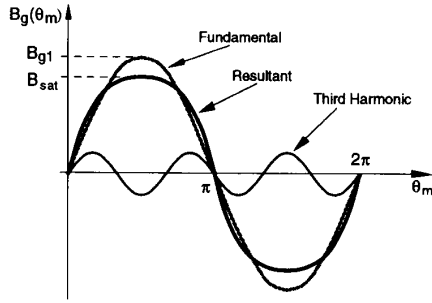


Fig. 1. Flux density distribution around the air gap of an induction machine (heavy line). Its fundamental and third harmonic components are also shown.

is balanced and operating in a normal balanced condition. Therefore, the third harmonic flux component rotates with the fundamental component, both at synchronous speed [10].

This synchronously rotating third harmonic flux density component will link the stator windings and a third harmonic voltage will be induced in each one of the phases. The third harmonic induced voltages are all in phase forming a zero sequence set and consequently the line voltages will be free of these components.

The amplitude of the induced third harmonic phase voltages is a function of the saturation level which is dictated by the amplitude of the fundamental component of the air gap flux for a given machine design. A more detailed analysis of the generation of the third harmonic stator voltage for a saturated machine is appropriate at this point. Taking into account only the fundamental and third harmonic components for the air gap flux density when the machine is under the saturation condition, and neglecting the influence of the rotor third harmonic currents, the resultant air gap field flux density,  $\mathbf{B}_{st}$ , is expressed by the vectorial sum of the three phase flux components according to:

$$\mathbf{B}_{st} = \mathbf{B}_{as} + \mathbf{B}_{bs} + \mathbf{B}_{cs} \quad (1)$$

or as derived in [9],

$$\begin{aligned} \mathbf{B}_{st} = & \frac{3}{2} \mu_0 k_e N_{s1} I_s \cos(\theta - \theta_e) \\ & - \frac{3}{4} \mu_0 k_m N_{s1} I_s [\cos(\theta - \theta_e) + \cos(3\theta - 3\theta_e)] \quad (2) \end{aligned}$$

Equation (2) above shows that the air gap field constitutes of two traveling waves: the fundamental component traveling in the air gap at synchronous frequency  $\omega_e$  and the third harmonic that travels at three times the synchronous frequency. The flux linking the stator phase *a*, for instance, is obtained from the integral of the product of the expression above by the stator phase-*a* winding function,  $N_{as}(\theta)$

$$\begin{aligned} \lambda_{as} = & \frac{3}{2} \mu_0 r l \left[ k_e N_{s1}^2 I_s \cos \theta_e - \frac{1}{2} k_m N_{s1}^2 I_s \cos \theta_e \right. \\ & \left. - \frac{1}{2} k_m N_{s1} N_{s3} I_s \cos 3\theta_e \right] \quad (3) \end{aligned}$$

Moreover, the phase voltage is given by

$$\begin{aligned} v_{as} = & \frac{3}{2} \mu_0 r l \left[ -\omega_e k_e N_{s1}^2 I_s \sin \theta_e + \frac{1}{2} \omega_e k_m N_{s1}^2 I_s \sin \theta_e \right. \\ & \left. + \frac{3}{2} \omega_e k_m N_{s1} N_{s3} I_s \sin 3\theta_e \right] \quad (4) \end{aligned}$$

where the following symbols are defined:

- $k_e$  constant related to the air gap length,
- $k_m$  constant related to the saturation level,
- $r$  air gap mean radius,
- $l$  equivalent machine stack length,
- $N_{s1}$  winding factor for the fundamental component of the winding function,
- $N_{s3}$  winding factor for the third harmonic component of the winding function,
- $I_s$  stator current amplitude,
- $\omega_e$  synchronous speed,
- $\theta_e$  electrical angle,
- $\theta$  angular position around the air gap.

It is evident from the expression above that the third harmonic voltage component of the stator phase voltage has a fixed phase relationship with the fundamental air gap flux and that its amplitude is a function of the amplitude of the fundamental flux component.

### III. ADAPTIVE CONTROLLER FOR THE ROTOR TIME CONSTANT BASED ON THE STATOR VOLTAGE THIRD HARMONIC CONTENTS

When the three stator phase voltages are summed, the fundamental and characteristic harmonics are cancelled and the resultant waveform contains mainly a third harmonic and high frequency components due to the inverter switching frequency and rotor slots. This resultant term is produced by the third harmonic of the air gap flux that maintains a constant position with respect to the fundamental flux component, and can be used to locate the position of the air gap flux, as well as to estimate its fundamental amplitude. The summation signal is a sine wave, practically free from the noise and fast transitions that characterize the line (or phase) voltage signals.

The amplitude of the fundamental component of the air gap flux,  $|\lambda_m|$ , is measured from the third harmonic component of the stator flux linkage obtained from an integration of the third harmonic stator voltage  $v_3$ . Thus, the amplitude of the fundamental component of the flux linkage is expressed in terms of the amplitude of the third harmonic flux component via a non-linear function,  $f_\lambda$ ,

$$|\lambda_m| = f_\lambda(|\lambda_3|) \quad (5)$$

Fig. 2 shows the relationship between the air gap fundamental flux component  $|\lambda_m|$  and the third harmonic flux component  $|\lambda_3|$  obtained from the stator third harmonic voltage, plotted here for the test induction machine described in Table I at the end of the paper. This function is derived from the conventional no-load test.

The position of the fundamental component of the air gap flux relative to the stator current is obtained by measuring the phase displacement between two fixed points in the third harmonic flux and line current. Fig. 3 shows this phase displacement represented by the symbol  $\gamma_{im}$  with the two reference points in the line current and third harmonic signal taken so that  $\gamma_{im}$  corresponds to the phase displacement between, for instance, the maximum values of current and air gap flux fundamental components.

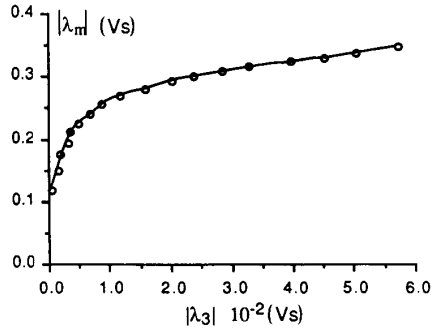


Fig. 2. Function relating the fundamental component of the airgap flux with the amplitude of the third harmonic flux component for the test machine.

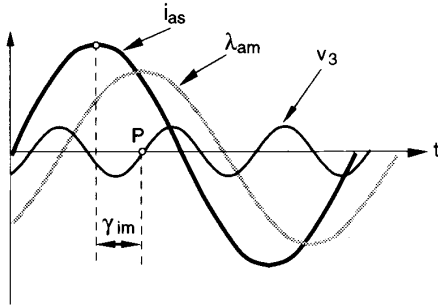


Fig. 3. Fundamental components of stator line current  $i_{as}$  and air gap flux fundamental ( $\lambda_{am}$ ) and third harmonic ( $\lambda_3$ ) components. The phase displacement for the stator current and air gap flux is represented by the angle  $\gamma_{im}$ .

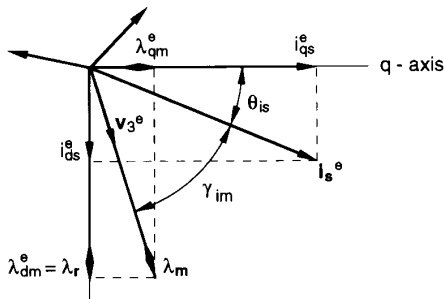


Fig. 4. Stator current, air gap flux, and third harmonic voltage vectors for a field orientation condition in the synchronous reference frame.

The fundamental and third harmonic components air gap flux, and the stator current are depicted in Fig. 4 in a synchronously rotating reference frame representation for a condition of field orientation. It is clear from this vector arrangement that the air gap flux can be resolved into its  $d$  and  $q$  components with the knowledge of its magnitude and the angles  $\gamma_{im}$  and  $\theta_{is}$ .

The  $d$ -axis component of the air gap flux, that corresponds to the rotor flux when the machine is field oriented, is then

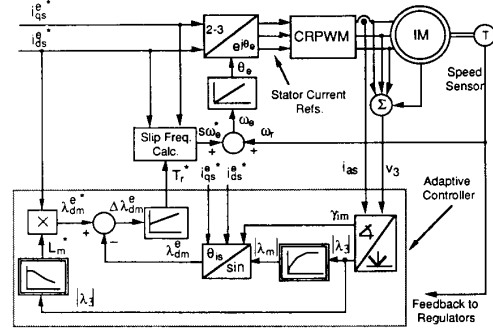


Fig. 5. Implementation for the rotor time constant correction scheme with correction for the magnetizing inductance estimate based on the amplitude of the third harmonic voltage signal.

computed as,

$$\lambda_{dm}^c = -|\lambda_m^c| \sin(\theta_{is} + \gamma_{im}) = -f_\lambda(|\lambda_3^c|) \sin(\theta_{is} + \gamma_{im}) \quad (6)$$

with  $\theta_{is}$  computed from the reference values (or actual measured values) of the stator currents,  $i_{qs}^c$  and  $i_{ds}^c$  as indicated by (7).

$$\theta_{is} = -\tan^{-1} \left( \frac{i_{ds}^c}{i_{qs}^c} \right) \quad (7)$$

The air gap flux  $d$ -axis component computed from (6) above is utilized by the adaptive controller which can be viewed as a Model Reference Adaptive Controller (MRAC) approach as presented in Fig. 5. The simplicity of the MRAC is the key point in this implementation. The controller only requires an estimate for the magnetizing inductance  $L_m^*$  in order to set the flux reference that, with the flux computed as in (6), define the flux error signal  $\Delta\lambda_{dm}^c$ . This error is driven to zero by the flux controller as the rotor time constant  $T_r^*$  is adjusted to its correct value. The simplicity achieved for the controller is possible only due to the choice for the model output chosen,  $\lambda_{dm}$  in this case.

In spite of the simplification obtained, the controller still depends on the magnetizing inductance, a parameter that varies with changes in the machine operating conditions. Changes in the magnetizing inductance are associated with the air gap flux level, which is a function of the stator current  $d-q$  components. Therefore, changes in the torque or flux commands will change the air gap flux level and consequently the magnetizing inductance, especially if the machine operates in the nonlinear segment of the magnetization characteristic curve.

Fortunately a function relating the actual value of the magnetizing inductance and the magnitude of the third harmonic flux component can be readily obtained from the the function relating the air gap flux amplitude and third harmonic flux amplitude described by  $f_\lambda$  in (5). Hence, a function, designated as  $f_{Lm}$ , is thus derived,

$$L_m = f_{Lm}(|\lambda_3|) \quad (8)$$

and Fig. 6 presents this function obtained experimentally from a no-load test for the test motor described in Table I.

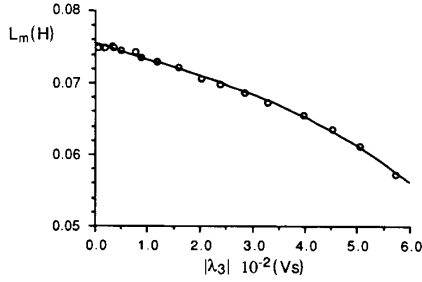


Fig. 6. Magnetizing inductance for the test machine as a function of the third harmonic flux signal amplitude.

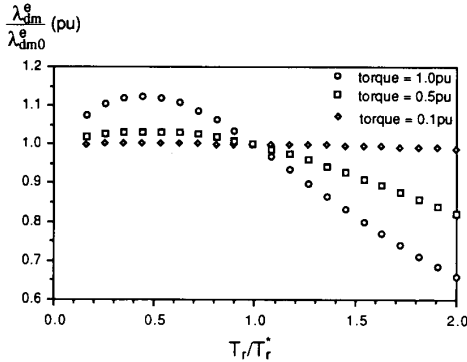


Fig. 7. Normalized *d*-axis component of the air gap flux versus normalized rotor time constant for the test motor.

This function relating  $L_m$  and  $|\lambda_3|$  is readily incorporated in the controller in Fig. 5 and the resulting adaptive control scheme becomes independent of variations of the magnetizing inductance caused by changes in the air gap flux level.

The performance of the MRAC can be evaluated from the curves presented in Fig. 7 that shows the steady-state value of the normalized *d*-axis component of the air gap flux as a function of the normalized detuning of the rotor time constant for the test motor. These quantities are normalized with respect to the values at ideal field orientation condition. Curves for three different values of torque at rated flux are plotted. The results show that the correct value of rotor time constant is always guaranteed since the  $\lambda_{dm}^c$  is not a doubly valued function and presents a zero flux error at the correct rotor time constant for all torque conditions. It is also possible to conclude from these results that the controller is always stable regarding the direction of change in the rotor time constant. A potential problem for this type of controller, however, is its low sensitivity to detuning for low torque conditions. The results in the figure show that a low sensitivity to detuning exists when the machine is running at 10% of the rated torque. This can represent a problem if a correct tuning is desired when operating at light load conditions. Increasing the controller gains, for instance, would be a possible solution for the low sensitivity problem. Caution have to be exercised in order not to compromise the dynamic response of the system.

The dynamic response of the MRAC is also sensitive to the operating condition of the system. Simulation and

experimental results show that the adaptive controller response is a function, for example, of the direction of change in the rotor time constant. This type of behavior can be explained by the fact that the MRAC, which is implemented with constant controller gains, is actuating in a non-linear system. Consequently, the eigenvalues of the system plus controller are space variant, changing as the operating conditions of the drive are changed.

In most practical applications the detuning of the slip calculator will be a result of changes in the rotor resistance that has a thermal time constant much larger than any electrical or mechanical time constants in the system. As a result the variant dynamic response of the controller will not necessarily be an issue to be concerned with if stability is guaranteed. Furthermore, the controller low sensitivity will not represent a problem in applications where the motor operates loaded during most of the operating cycle.

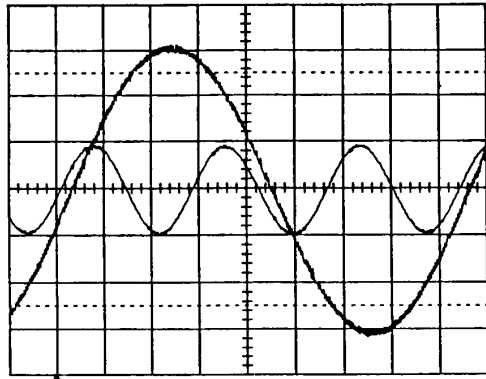
IV. SIMULATION AND EXPERIMENTAL RESULTS

Experimental results demonstrating the feasibility of the concept of locating the air gap flux via third harmonic stator voltage, and its utilization in implementing the proposed adaptive controller have been obtained in the laboratory. Fig. 8 shows the third harmonic stator voltage signal obtained from the summation of the three phase voltages for operation at no load and synchronous frequency around 30 Hz. A current regulated PWM inverter is used to supply the induction machine. Fig. 8(a) shows the third harmonic voltage and one of the line currents. The switching frequency component in the third harmonic voltage is eliminated by a low pass filter (LPF) making this signal convenient for an analog or digital manipulation. Another LPF is used for the current so that the phase displacement between the current and third harmonic voltage is kept at its original value.

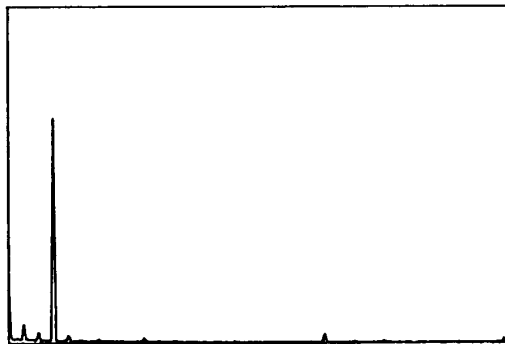
The third harmonic frequency spectrum is analyzed and shown in Fig. 8(b). As predicted, after the summation of the three phase voltages all the polyphase components (fundamental, 5<sup>th</sup>, 7<sup>th</sup>, 11<sup>th</sup>, and so forth) are eliminated and the third harmonic is clearly the dominant component at the lower side of the frequency spectrum.

A digital simulation of the adaptive controller shown in Fig. 5 has been carried out to verify the validity of the rotor time constant adaption method. In particular, a delta-current regulated PWM inverter and an indirect field orientation control algorithm have been implemented. The induction machine model includes effects of saturation and also makes provision for the existence of third harmonic stator voltages. Neither speed nor position feedback control is assumed so that the effects of detuning in the torque response can be fully investigated.

The simulation results in Fig. 9 show the evolution from bottom to top of the rotor time constant reference value, air gap *d*-axis component, error in the air gap flux *d*-axis component, rotor *q*-axis component, and motor torque. The trace shows the transient that occurs for an increase of 100% in the rotor resistance at time equals to 1.0 s. These results show that the machine is working essentially under field orientation



(a)



(b)

Fig. 8. Experimental results obtained for the test machine. (a) Line current (upper trace: 5 A/div) and stator third harmonic voltage (bottom trace: 5 V/div). (b) Third harmonic voltage spectrum (full scale of 9 V/rms).

condition up to the instant when the disturbance occurs in the rotor resistance. As soon as the disturbance occurs the rotor and the air gap flux increase as a consequence of the over excitation produced by the increase in the rotor resistance. The adaptive controller starts then to command the rotor time constant to its new value while driving the air gap flux error to zero. After approximately 1.7 s the machine regains the condition of field orientation when the rotor time constant reaches its correct value, while the  $q$ -axis component of the rotor flux becomes zero.

An indirect rotor flux orientation scheme was implemented using a Motorola DSP 56001 development system. A simple hysteresis regulator was digitally implemented to provide the current regulation for the three stator currents. The motor used in the experimental set up is a wound rotor three phase induction machine described in Table I. The motor was installed in a dynamometer and an incremental shaft encoder used for position detection. An external three phase resistance network was connected to the rotor terminals so that the actual rotor resistance could be increased to about twice its nominal value.

The operation of the MRAC correcting variations of the actual rotor resistance is verified in the laboratory and plotted in Fig. 10. Rated torque and flux commands are used. A step change in the rotor resistance from nominal to twice nominal

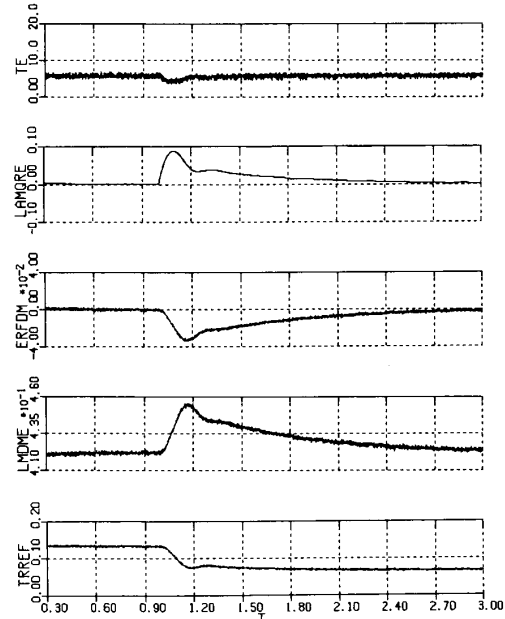


Fig. 9. Simulation results for the rotor time constant adaption scheme as proposed in Fig. 7 running at rated torque and flux.

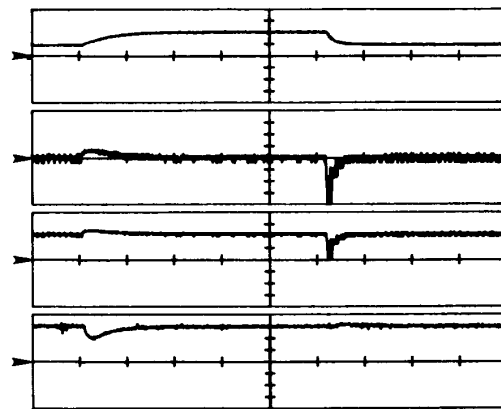


Fig. 10. Experimental results for the MRAC. From bottom to top: i) speed (150 rpm/div), ii)  $d$ -axis air gap flux (0.2 V.s/div), iii) flux error (0.2 V.s/div), and iv) slip gain (10 Hz/A/div); Hor: 5 s/div.

is applied to the motor by changing the external resistance connected to the rotor terminals. After the system response to this change, another step change is applied so that the nominal rotor resistance is reestablished.

It is clear from Fig. 10 that the correction action of the adaptive controller has different dynamics when the rotor resistance is decreased to its nominal value. As predicted from Fig. 7 the error in flux is larger when the rotor resistance gets lower than its estimate. The non-linear behavior of the system is also made clear by the type of response to the reduction of the rotor resistance. The system in this case is able to correct the slip gain in about 2 s, and almost no speed transients are observed.

TABLE I  
INDUCTION MACHINE PARAMETERS

Quantity	Symbol	Value
Line Voltage	$V_1$	220 V <sub>rms</sub>
Output	Power $P_0$	1/3 HP
Speed	$\omega_r$	1725 rpm
Poles	$P$	4
Stator Resistance	$r_s$	7.15 $\Omega$
Rotor Resistance	$r_r$	6.0 $\Omega$
Stator Leakage Reactance	$X_{l_s}$	5.14 $\Omega$
Rotor Leakage Reactance	$X_{l_r}$	3.23 $\Omega$
Unsat. Magnetizing Reactance	$X_m$	100.65 $\Omega$
Motor Inertia	$J_m$	0.022 Kg-m <sup>2</sup>

## V. CONCLUSION

A new and simple method for correcting the rotor time constant in Indirect Field Oriented Control of induction machines is proposed in this work. The method is based on the measurement of the air gap flux from the third harmonic component of stator voltage. It is shown that due to the machine saturation the air gap flux contains a strong content of third harmonic which induces a third harmonic voltage in the stator phases. A predominant third harmonic voltage component is obtained when the three stator phase voltages are summed as a consequence of the elimination of the polyphase fundamental and harmonic components. The resulting signal has the advantage of having low levels of noise and high frequency content.

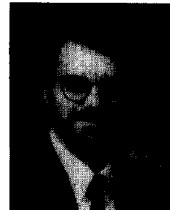
The third harmonic component is then used to determine the position of the fundamental component of the air gap flux. The air gap flux is resolved in its  $d$  and  $q$ -axis components from the third harmonic and line current signals. The  $d$ -axis component of the flux is used as a control signal for the adaptation of the rotor time constant. The adaptive controller proposed can be viewed as a Reference Model (MRAC) type where only an estimate of the magnetizing inductance of the machine is necessary for implementation. Furthermore, a correction strategy for changes in the magnetizing inductance based on the amplitude of the third harmonic flux signal is also implemented in the controller. This addition is important since the magnetizing inductance is a sensitive parameter in terms of the air gap flux level, that is a function of load and flux reference conditions.

Experimental and simulation results have proven the feasibility of utilizing the stator third harmonic voltage contents to locate the air gap flux and the practicality of the adaption scheme proposed. Despite the low sensitivity for low torque output and varying dynamics, this MRAC presents a very attractive characteristic of being practically independent of machine parameters. The only machine data needed for its implementation is the function  $f_{Lm}$ . The result is a controller with a high robustness relative to the machine parameters. Experimental results have shown that the controller is capable of estimating the right air gap flux value for a wide range of speed.

## REFERENCES

- [1] R. D. Lorenz, "A Simplified Approach to Continuous, On-Line Tuning of Field Oriented Induction Machine Drives", in *1988 IEEE-IAS Annu. Meet. Conf. Rec.*, pp. 444-449.

- [2] T. M. Rowan, R. J. Kerkman and D. Leggate "A Simple On-Line Adaption for Indirect Field Orientation of an Induction Machine", in *1989 IEEE-IAS Annu. Meet. Conf. Rec.*, pp. 579-587.
- [3] S. K. Sul, "A Novel Technique of Rotor Resistance Estimation Considering Variation of Mutual Inductance", in *1987 IEEE-IAS Annu. Meet. Conf. Rec.*, pp. 184-188.
- [4] H. Sugimoto and S. Tamai, "Secondary resistance identification of an induction-motor applied model reference adaptive system and its characteristics", in *IEEE Trans. on Ind. Appl.*, vol. IA-23, pp. 296-303, 1987.
- [5] L. C. Zai and T. A. Lipo, "An extended kalman filter approach to rotor time constant measurement in pwm induction motor drives", in *1987 IEEE-IAS Annu. Meet. Conf. Rec.*, pp. 177-183.
- [6] T. Matsuo and T. A. Lipo, "A rotor parameter identification scheme for vector-controlled induction motor drives", in *IEEE Trans. Industry Applicat.*, vol. IA-21, pp. 624-632, 1985.
- [7] L. J. Garces, "Parameter adaption for the speed-controlled static ac drive with a squirrel-cage induction motor," in *IEEE Trans. Industry Applicat.*, vol. IA-16, pp. 173-178, 1980.
- [8] J. C. Moreira, T. A. Lipo, and V. Blasko, "Low cost efficiency maximizer for an induction motor drive," in *1989 IEEE-IAS Annual Meet. Conf. Rec.*, pp. 426-431 (to appear in the *IEEE Trans. Industry Applicat.*).
- [9] J. C. Moreira, "A study of saturation harmonics with applications in induction motor drives," *Ph.D. Thesis*, Univ. Wisconsin-Madison, Sept. 1990.
- [10] C. H. Lee, "Saturation harmonics of polyphase induction machines," in *AIEE Transactions*, vol. 80, part III, pp. 597-603, October 1961.
- [11] N. L. Schmitz and D. W. Novotny, *Introductory Electromechanics*. New York:Ronald Press, 1965.
- [12] G. H. Rawcliffe and B. C. McDermott, "The theory of third-harmonic and zero sequence fields," in *IEE - Monograph*, N° 157U, Dec. 1955.
- [13] F. Blaschke, "Das Verfahren der Feldorientierung zur Regelung der Drehfeldmaschine" ("The method of field orientation for control of three phase machines"), *Ph.D. dissertation*, Institut für Regelungstechnik, Technische Universität Braunschweig, 1974.
- [14] K. Hasse "Zur Dynamic Drehzahlgeregelter Antriebe mit Stromrichter gespeisten Asynchron-Kurzschlusslaufmaschinen" ("On the dynamics of speed control of a static ac drive with squirrel-cage induction machine"), *Ph.D. dissertation*, Technische Hochschule Darmstadt, 1969.
- [15] K. J. Åström and B. Wittenmark, *Computer Controlled Systems - Theory and Design*. New York:Prentice-Hall, 1984.



**Julio C. Moreira** (S'81-M'90) was born in Sao Paulo, Brazil, where he received the B.S. and M.S. degrees in electrical engineering from the State University of Campinas (UNICAMP) in 1979 and 1983, respectively. He received the Ph.D. degree in electrical engineering from the University of Wisconsin, Madison, in 1990.

He worked as an Engineer and later as a Vice-Coordinator of the Electric Drive Systems Research Laboratory at the State University of Campinas in Brazil from 1980 to 1985. In 1981 he became a Researcher and an Assistant Professor at that same institution, teaching courses in Electrical Machines, Power Electronics, Industrial Electronics, Servo Drive Controls and Microprocessors. His research activities included the development of dc and ac motor drives systems for public transportation and for electric vehicles. He also served as a consultant in the areas of Electric Drive Systems and Switched Mode Power Supplies. After receiving the Ph.D. he joined the Whirlpool Corporate Research and Engineering Center, Michigan, as a Lead Engineer where he is involved with research in the areas of Power Electronics, Electric Machines Design, Electric Motor Drive Systems, and Digital Controls. He has received two IEEE prize paper awards and two U.S. patents pending.

Dr. Moreira is a member of IEEE Power Electronics Society, the IEEE Industry Applications Society and the IEEE Industrial Electronics Society.

**Thomas A. Lipo**, photograph and biography not available at the time of publication.